

Photoelectrochemical Properties of TiO₂ Films Prepared by the Sol-Gel Method

Toshinobu YOKO, Kanichi KAMIYA and Sumio SAKKA*

(Department of Industrial Chemistry, Faculty of Engineering, Mie University
Kamihama-cho, Tsu-shi, Mie 514)

*Institute for Chemical Research, Kyoto University

ゾル・ゲル法により調製した TiO₂ 薄膜の光電気化学的性質

横尾 俊信・神谷 寛一・作花 濟夫*

(三重大学 工学部 工業化学科)

*京都大学 化学研究所

TiO₂ films of more than 2 μm thick which are an n-type semiconductor have been prepared on a nesa glass substrate by a dip-coating technique using TiO₂ sol solution. Heating temperature of 500°C was adopted to convert TiO₂ gels into TiO₂ (anatase) crystalline films. The TiO₂ films show a maximum photocurrent (~14 mA cm⁻²) at the film thickness of about 1.8 μm. It is also found that the additional heating at 500°C improves remarkably the photocurrent of the TiO₂ films, although too long heating rather deteriorates it. These results are explained on the basis of the changes in both the surface structure and carrier concentration of the films with the additional heating time. [Received July 11, 1986]

Key-words : Photoelectrochemistry, Sol-gel method, TiO₂ film, n-type semiconductor, Solar energy conversion, Anatase

1. Introduction

TiO₂ of n-type semiconductor has been of great interest as a material for solar energy conversion, since Fujishima et al.¹⁾ found that it can decompose water without any deteriorations under illumination. TiO₂ (rutile) single crystal was originally used as a photoanode. It is, however, too expensive for practical applications. This is also the case for the sintered polycrystalline bodies.

In order to overcome this problem, many attempts have been made to prepare thin TiO₂ films for a photoanode, for example, by chemical vapor deposition (CVD)²⁾⁻⁴⁾, anodization and thermal oxidation of Ti metal⁵⁾⁻⁸⁾ and dip-coating from TiO₂ sol solution⁹⁾. It should be mentioned here that the last method was first applied for sun-shielding pane by Dislich and Hussman¹⁰⁾.

The present paper will deal with the photoelectrochemical properties of TiO₂ films in the anatase form prepared by the sol-gel method. In particular, the effect of heat treatment on the photocurrent of TiO₂ film electrode will be discussed in detail.

2. Experimental

2.1 TiO₂ film preparation

TiO₂ sol solution was prepared by mixing Ti

(O-i-C₃H₇)₄, anhydrous C₂H₅OH and H₂O as shown in Fig. 1. Half of the prescribed amount of anhydrous C₂H₅OH was added slowly to Ti(O-i-C₃H₇)₄ which was cooled with ice and stirred. The rest of anhydrous C₂H₅OH is mixed with H₂O and HCl as a catalyst. The C₂H₅OH-H₂O-HCl solution is added dropwise to the Ti(O-i-C₃H₇)₄-C₂H₅OH solution with a buret

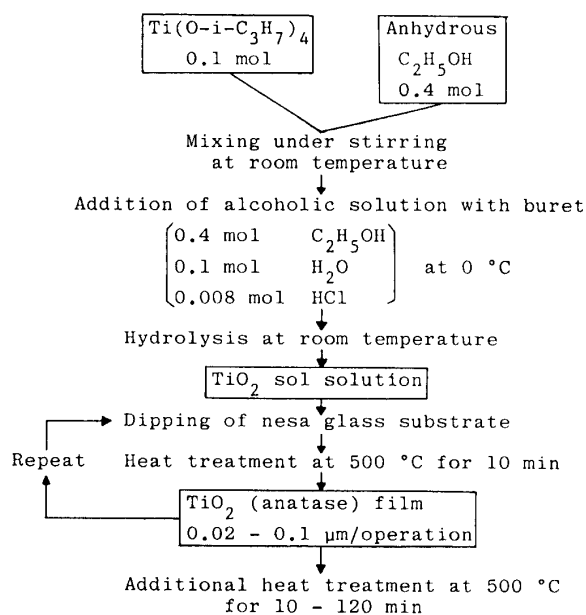


Fig. 1. Preparation process of the TiO₂ film on nesa glass substrate.

under stirring. The chemical composition of the starting alkoxide solution prepared in the present work is also shown in Fig. 1.

TiO₂ gel films were obtained by dipping nesa glass substrate in the TiO₂ sol solution and subsequently pulling it up at constant speed ($\sim 0.15 \text{ mms}^{-1}$) using an apparatus shown in Fig. 2. The TiO₂ gel films thus obtained were subjected to heat treatment at 500°C for 10 min. By repeating the above operations, TiO₂ films up to about 2 μm thick could be obtained.

2.2 Photoelectrochemical measurements

Photoelectrochemical behavior of the TiO₂ film electrode was determined in 0.1 N H₂SO₄ solution using a potentiostat with three electrodes as shown in Fig. 3; besides TiO₂ photoelectrode Pt plate of 35 \times 25 mm and SCE were employed as a counter electrode and a reference electrode, respectively. A 500 W Xenon lamp was used to illuminate the TiO₂ electrode. Impedance analysis for the TiO₂ film electrode was also performed using a lock-in amplifier at a fixed frequency (1015 Hz).

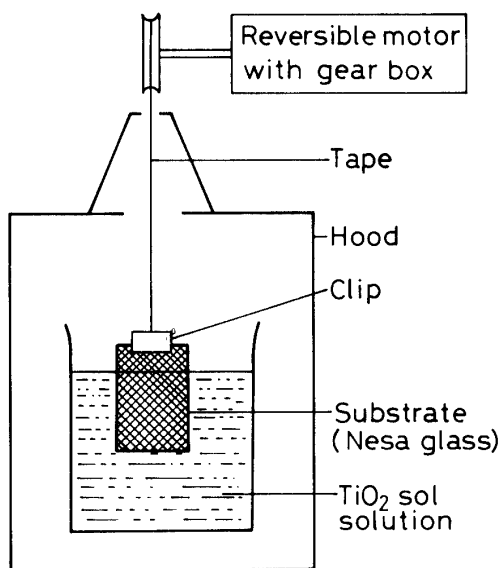


Fig. 2. Apparatus for dip-coating.

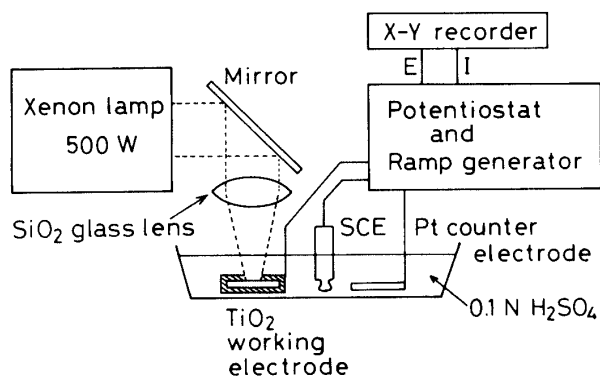


Fig. 3. Schematic diagram for measuring photoelectrical current.

3. Result

3.1 Thickness and coloration of TiO₂ film

Figure 4 shows a linear relation between the TiO₂ film thickness and the number of application of the sol. The average film thickness per application is estimated to be about 0.09 μm at the pulling speed of 0.15 mms^{-1} . The film thickness was measured using a profilometer with a diamond stylus.

The TiO₂ film thus prepared shows coloration phenomenon¹¹⁾. The color strongly depends on the film thickness and those by transmitting and reflecting light are complementary each other. As the thickness of TiO₂ film increases up to more than 1 μm , the coloration becomes indistinct, while the films remain still transparent. Therefore, it can be concluded from these results that the coloration is caused by the interference of light.

3.2 Transformation of TiO₂ gel into crystalline form

A typical DTA curve of TiO₂ gel powders is shown in Fig. 5. A broad endothermic peak between 100° and 200°C and a relatively sharp exothermic peak at 258°C are due to dehydration and combustion of organic substances contained in the gel, respectively, although their positions

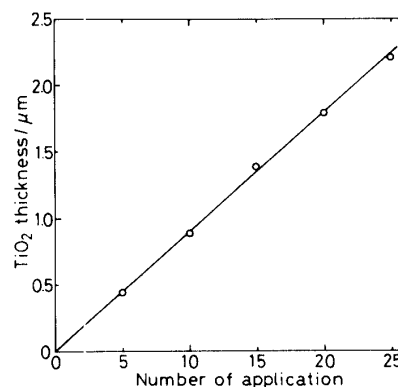


Fig. 4. Relation between the TiO₂ film thickness and the number of application of the sol.

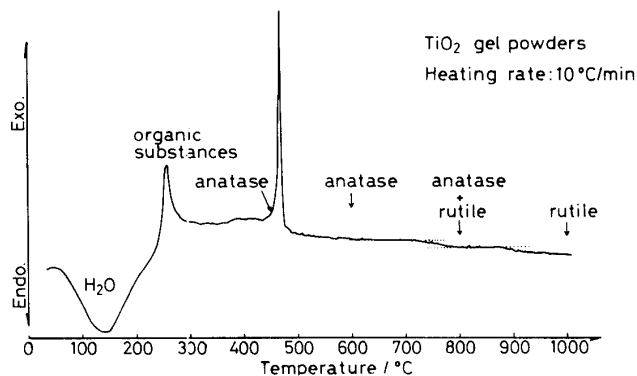


Fig. 5. A typical DTA curve of TiO₂ gel powders.

and intensities are strongly dependent on the gel preparation process.

According to X-ray diffraction analysis, anatase crystal formation was found to begin at around 450°C. At 468°C a very sharp exothermic peak was observed due to anatase crystal formation. A part of anatase crystal started to transform into rutile crystal at around 720°C. On further heating up to 1000°C, only rutile crystal was observed.

Similarly to the TiO₂ gel powders, the TiO₂ gel films coated on the nesa glass were found to transform into anatase crystal on heating at 500°C. Because of the lack of the heat-resistance of nesa glass used, the heating temperature more than 500°C was not attainable. Therefore, the TiO₂ film of rutile crystal was not used as a photoelectrode in the present study.

3.3 Photoelectrochemical (PEC) behavior of TiO₂ film electrode

Figure 6 shows polarization curves of TiO₂ film electrodes with different thicknesses taken at scan

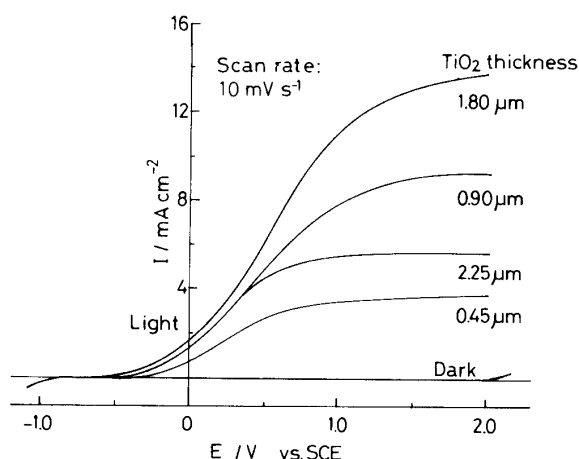


Fig. 6. Polarization curves of TiO₂ film electrode with different thicknesses.

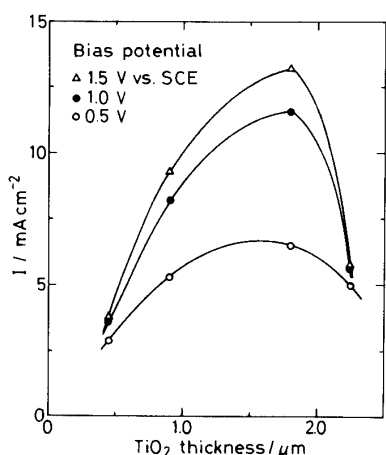


Fig. 7. Variations of photocurrent with the TiO₂ film thickness at several bias potentials (vs. SCE).

rate of 10 mVs⁻¹ under and without illumination. Without illumination it is not until the potential reaches about 2 V (vs. SCE) irrespective of the film thickness that the current probably due to oxygen evolution becomes detectable. On the other hand, under illumination the PEC current starts to flow at around -0.3- -0.5 V (vs. SCE) and shows a plateau at around 0.5-1.0 V (vs. SCE), where vigorous evolution of gases was observed on the both TiO₂ anode and Pt cathode. The PEC behaviors observed for TiO₂ film electrode are quite similar to that for single crystal TiO₂ electrode¹⁾, although the present TiO₂ film electrode is in the anatase form as previously described.

It is also clearly seen from Fig. 6 that the PEC currents strongly depend on the film thickness. Figure 7 shows the variations of the PEC current with the TiO₂ film thickness at bias potentials of 0.5, 1.0 and 1.5 V (vs. SCE), respectively. At any bias potentials the PEC current increases with increasing film thickness, reaches a maximum at about 1.8 μm and then falls with further increase in the film thickness. It is noteworthy that the TiO₂ (anatase) film electrode of 1.8 μm thick shows a maximum PEC current as high as 14 mAcm⁻² at the bias potential above 1.5 V (vs. SCE), which is comparable to or slightly higher than the values reported for single crystal and polycrystalline TiO₂, and much higher than those for the TiO₂ film electrode prepared by other methods such as CVD^{2),4)}, oxidation^{5),8)} and anodization⁷⁾ of Ti metal.

3.4 Effect of additional heating (AH) on the PEC behavior of as-prepared TiO₂ film electrode

Figure 8 shows polarization curves for TiO₂ film electrode of 0.9 μm thick which was sub-

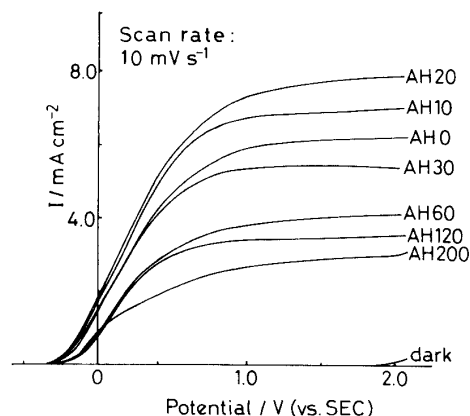


Fig. 8. Polarization curves of TiO₂ film electrode subjected to additional heating for various time periods at 500°C.

jected to the additional heating for various time periods from 10 to 120 min. As can be clearly seen from the figure, the PEC behavior is greatly dependent on the AH time. Although the onset potentials do not shift appreciably, the slope of current rise becomes steeper and the saturation current increases with increasing AH time up to 20 min, and then both of them decrease with further increase in the AH time. **Figure 9** shows the variations of photocurrent at bias potentials of 0.0, 0.5 and 1.0 V (vs. SCE) with the AH time. It is quite noteworthy that the photocurrents at all the bias potentials are found to give a maximum at the AH time of about 20 min.

4. Discussion

4.1 Film thickness dependence of photocurrent of the as-prepared TiO₂ films

It is generally known that the space charge layer at the semiconductor surface in contact with electrolyte, where the separation of electrons and holes takes place under illumination, is 0.1-1000 μm , depending on the carrier concentration¹²⁾. In the present study as shown in Figs. 6 and 7, the TiO₂ film electrode shows a maximum photocurrent at the film thickness of about 1.8 μm , although the photocurrent should be expected to increase with increasing film thickness because a

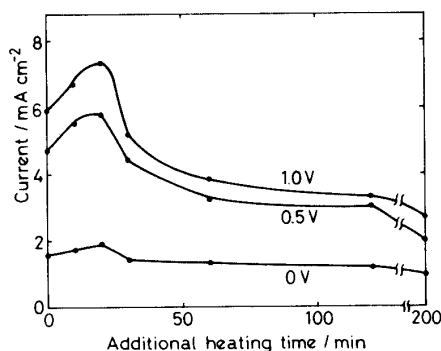


Fig. 9. Variations of photocurrent of TiO₂ film electrode with the additional heating time (AH time).

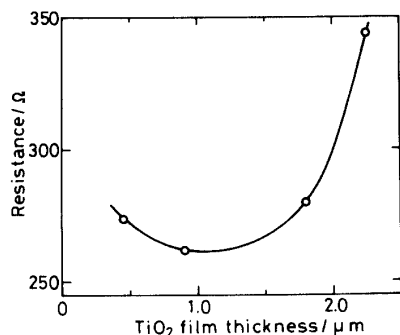


Fig. 10. Variation of resistance of TiO₂ film electrode with the thickness.

film thickness of about 1 μm is considered to be of the order of the space charge layer thickness.

In order to make this point clear, the impedance analysis¹³⁾ has been conducted for the TiO₂ film electrode. **Figure 10** shows a variation of the resistance of TiO₂ film electrode with thickness, which was determined by assuming a simple equivalent circuit consisting of series of bulk resistance and space charge layer capacitance. The resistance does not change significantly up to about 1.8 μm but increases sharply above it. Higher bulk resistance causes a larger voltage drop, resulting in a promotion of the recombination of photogenerated electrons and holes in the space charge layer due to a decrease in the potential gradient across it¹⁴⁾. It is, therefore, concluded that the decrease in photocurrent of TiO₂ film electrode above about 1.8 μm thick is mainly ascribed to an increase in the resistance.

Figure 11 shows the variations of the flat band potentials V_{fb} determined by the Mott-Schottky plot¹³⁾ under illumination and in the dark, and their difference ΔV_{fb} (the flat band shift) with film thickness. The behavior of ΔV_{fb} is quite similar to that of photocurrent in Fig. 7. That is, the larger the ΔV_{fb} , the larger the photocurrent. This reason will be discussed in the next section.

4.2 AH time dependence of photocurrent of the as-prepared TiO₂ films

It has been found that the photocurrent of the as-prepared TiO₂ film electrode of 0.9 μm thick increases with increasing AH time, reaches a maximum at the AH time of 20 min and then decreases with further AH time. The impedance

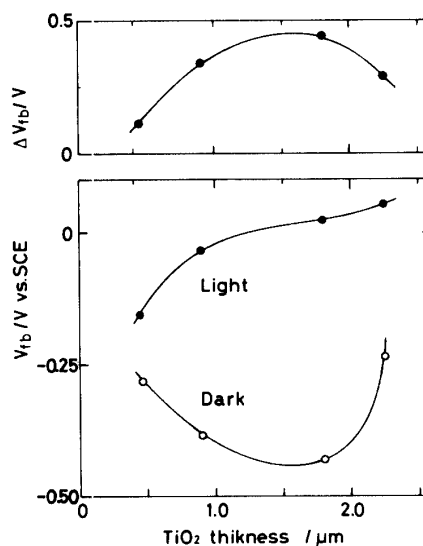


Fig. 11. Variations of V_{fb} and ΔV_{fb} obtained from the Mott-Schottky plot with the thickness for TiO₂ film electrode.

analysis was also performed in this case as in the previous section. The plot of the resistance of the TiO_2 film electrode vs. the AH time (Fig. 12) shows a minimum at 20 min, corresponding to the maximum in photocurrent (Fig. 7). This is also the case for the plots of the donor density (Fig. 13) and the ΔV_{fb} (Fig. 14) vs. the AH time.

The occurrence of a minimum in the resistance

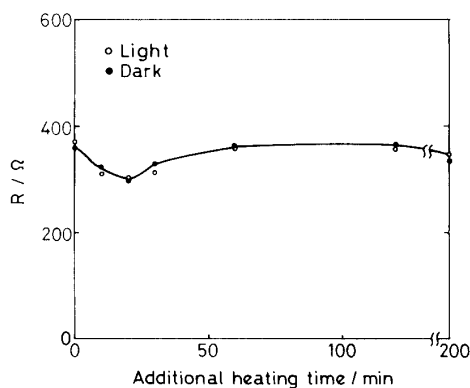


Fig. 12. Variation of resistance of the TiO_2 film electrode with the additional heating time.

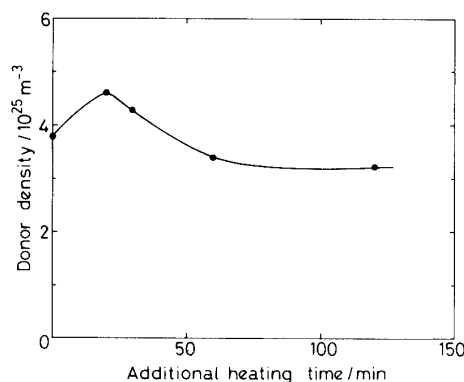


Fig. 13. Variation of donor density of TiO_2 film electrode with the additional heating time.

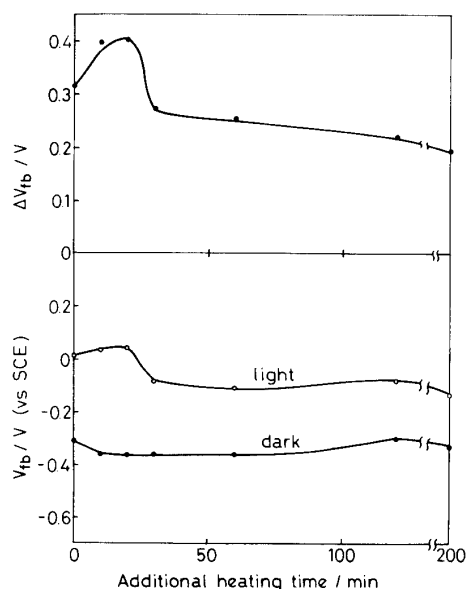


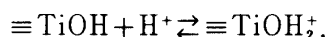
Fig. 14. Variations of V_{fb} and ΔV_{fb} for TiO_2 film electrode with the additional heating time.

of the TiO_2 film at a certain AH time may be explained as follows. It is well known that a resistance of semiconductor is controlled by charge carriers of electrons and/or holes. Since TiO_2 is an n-type semiconductor, the concentration of Ti^{3+} in TiO_2 which forms a donor level between the band gap of TiO_2 should govern the resistance of TiO_2 . The decrease in the resistance of TiO_2 films with the AH time is due to the increase in donor density occurring as a result of reduction of Ti^{4+} to Ti^{3+} by organic residue such as alcohol and unhydrolyzed alkoxide groups. However, once it is used up for the reduction of Ti^{4+} or burnt out on further heating in air, the donor density starts to decrease due to reoxidation of Ti^{3+} , resulting in the increase in the resistance.

As stated above, an increase in the bulk resistance of the semiconductor electrode causes a reduction of photocurrent and, on the contrary, a decrease in the bulk resistance of the semiconductor electrode results in an increase in the photocurrent due to the reduction of the recombination of photogenerated electrons and holes due to a decrease in potential drop across the space charge layer. Therefore, the maximum in photocurrent is possibly related to the minimum resistance of the TiO_2 film. It should be noted here that too low resistance, on the contrary, decreases a photocurrent due to a decrease in the space charge layer thickness, and consequently a decrease in effective photon absorption within the space charge layer⁽⁴⁾.

Moreover, the surface structure of TiO_2 film must be taken into account. The space charge layer thickness calculated from the slope of the Mott-Schottky plot is of the order of 10-20 nm, which is too thin compared with the generally expected value as stated previously. This probably reflects a large surface area of the sol-gel derived TiO_2 film resulting from its porous structure, because a smaller surface area than the actual one provides too thin space charge layer thickness in the calculation. Accordingly, the decrease in photocurrent above AH time of 20 min may be ascribed to both the reduction of carrier concentration due to the reoxidation of Ti^{3+} and the disappearance of porous structure.

The coincidence between the maxima in photocurrent and ΔV_{fb} may be explained as follows. In acidic solution of pH=1, the surface of TiO_2 film is in equilibrium with solution in the followings,



Photooxidation of water has been recently proposed to take place mainly via $\equiv\text{TiOH}_2^+$ in the acid solution¹⁵⁾. Nevertheless, there are also present OH_{aq}^- groups adsorbed on the TiO_2 , which fill the extrinsic surface states of TiO_2 ¹⁶⁾. Although these surface states may not be a major origin for the evolution of O_2 ¹⁶⁾, photogenerated holes can be trapped by this surface state, causing a positive flat band shift in the TiO_2 film electrode. This suggests that the larger the surface area, the more the surface states (defects), and consequently the larger the flat band shift becomes. It may be, therefore, concluded that up to the AH time of 20 min at 500°C, some alkoxide groups still remain and continue to decompose at the surface, leaving surface defects behind, which act as surface states.

5. Summary

TiO_2 films up to about 2 μm thick have been prepared on a nesa glass substrate by dip-coating technique using the TiO_2 sol solution derived from $\text{Ti}(\text{O}-i\text{-C}_3\text{H}_7)_4$. Photoelectrochemical properties of the TiO_2 film electrode thus obtained have been investigated as a potential candidate for solar energy conversion device. The results obtained are summarized as follows:

(1) The sol-gel derived TiO_2 film shows a very large photocurrent due to porous surface structure and a maximum ($\sim 14 \text{ mA cm}^{-2}$) at about 1.8 μm in thickness. A decrease in the photocurrent of the TiO_2 film above 1.8 μm thick is due to an increase in the resistance.

(2) An additional heating at 500°C improves remarkably the photocurrent of the TiO_2 film,

although too long heating rather deteriorates it. These results are explained on the basis of the changes in the surface structure and carrier concentration with the additional heating time.

Acknowledgement This work was supported by a Grant-in-Aid for Scientific Research from the Ministry of Education, Science and Culture.

References

- 1) A. Fujishima, K. Honda and S. Kikuchi, *Kogyo-Kagaku Zasshi*, **72**, 108-13 (1969).
- 2) F. Möllers, H. J. Tolle and R. Memming, *J. Electrochem. Soc.*, **121**, 1160-67 (1974).
- 3) E. T. Fitzgibbons, K. J. Sladek and W. H. Hartwig, *ibid.*, **119**, 735-39 (1972).
- 4) K. L. Hardee and A. J. Bard, *ibid.*, **122**, 739-42 (1975).
- 5) A. Fujishima, K. Kohayakawa and K. Honda, *J. Electrochem. Soc.*, **122**, 1487-89 (1975).
- 6) J. Augustynski, J. Hinder and C. Stalder, *ibid.*, **124**, 1063-64 (1977); C. Stalder and J. Augustynski, *ibid.*, **126**, 2007-11 (1979).
- 7) H. Tamura, H. Yoneyama, C. Iwakura and T. Murai, *Bull. Chem. Soc. Jpn.*, **50**, 753-54 (1977).
- 8) Y. Matsumoto, J. Kurimoto, Y. Amagasaki and E. Sato, *J. Electrochem. Soc.*, **127**, 2148-52 (1980); Y. Matsumoto, J. Kurimoto, T. Shimizu and E. Sato, *ibid.*, **128**, 1040-44 (1981).
- 9) T. Yoko, K. Kamiya and S. Sakka, *Denki-Kagaku*, **54**, 284-85 (1986).
- 10) H. Dislich and E. Hussman, *Thin Solid Films*, **77**, 129-39 (1981).
- 11) K. Kamiya and T. Yoko, *Hyomen*, **24**, 131-42 (1986) (in Japanese).
- 12) H. Tsubomura, "Photoelectrochemistry and Energy Conversion", Tokyo Kagaku Dozin (1979) Chap. 6 (in Japanese).
- 13) S. R. Morrison, "Electrochemistry at Semiconductor and Oxidized Metal Electrodes", Plenum Press (1980) Chap. 4.
- 14) R. H. Wilson, *J. Appl. Phys.*, **48**, 4292-97 (1977).
- 15) T. Yoko, K. Kamiya, A. Yuasa and S. Sakka, submitted to *J. Electroanal. Chem.*
- 16) P. Salvador, *J. Phys. Chem.*, **89**, 3863-69 (1985).